

Competitive binding of Activator-Repressor in Stochastic Gene Expression

Amit Kumar Das^{1,2,*}, Debabrata Biswas^{1†}

¹Department of Physics, Bankura University, Bankura-722 155, West Bengal, India.

²Digsui Sadhana Banga Vidyalaya, Digsui, Hooghly-712148, West Bengal, India.

Abstract

In this paper, we explore the features of a genetic network where the transcription factors (TFs), namely, activators and repressors bind to the promoter in a *competitive way*. We have developed an analytical method to find the most probable set of parameter values that are unavailable in experiments. We study the noisy behavior of the circuit and compare the profile with the network where the activator and the repressor bind the promoter *non-competitively*. We observe that the noise found in the super-Poissonian region of the competitive genetic circuit is higher than the noise obtained in the same from a non-competitive one. We further notice that, due to the effect of transcriptional reinitiation in the presence of the activator and repressor molecules, there exist some anomalous characteristic features in the mean expressions and noise profiles. On top of that, we find low noise in the transcriptional level and high noise in the translational level in presence of reinitiation than in absence of the same. In addition, we find out the method to reduce the noise further below the Poissonian level in competitive circuit than the non-competitive one with the help of some noise-reducing factors.

Keywords: Stochastic process, Gene Expression, Transcription factor, The Fano factor, reinitiation, Poissonian level, Competitive and non-competitive architecture

1 Introduction

Over the years, it has been experimentally verified and accepted that the gene expression regulation is an inherent stochastic process [1–11]. In parallel with the experiments, many theoretical approaches, analytical and numerical simulations, have been proposed in support [12–22]. Regulation of gene expression (GE) is essential for all organisms to develop their ability to respond to the environmental changes. It involves several complex stochastic mechanisms such as transcription, pre-initiation, reinitiation, translation, and degradation, etc. [23, 24]. Transcription is the initial step through which the biological information is being transferred from the genome to the proteome [25]. The regulation of transcription [18, 19] occurs whenever some regulatory proteins called transcription factors (TFs) interact with the promoter of a gene. Based on functionality, TFs are classified as activators and repressors in both prokaryotes and eukaryotes [25–27]. Repressors inhibit the gene transcription by binding to specific DNA sequences. Tryptophan and Lac are some widely known

*mr.das201718@yahoo.com

†debbisrs@gmail.com

repressors for prokaryotic systems. On the other hand, activators allow RNA-Polymerase (RNAP) to bind to the promoter and initiate the transcription, resulting in synthesizing mRNA. The molecular concentrations of these activators and/or repressors can be varied with the help of some inducer molecules, such as doxycycline (dox), galactose (GAL), tetracycline (Tc) and anhydrotetracycline (aTc), etc. [3, 10, 11].

An eukaryotic system is much more complex and possesses a compact chromatin structure than prokaryotes. In the eukaryotic system, a basic example of transcriptional regulation by TFs is a two-state telegraphic model [14, 15, 17], where a gene can be active (ON) or inactive (OFF) depending on whether TFs are bound to the gene or not, respectively. An active gene transcribes through the production of messenger-RNA (mRNA) in a pulsatile fashion during short intense periods known as transcriptional bursts, followed by a longer period of inactivity. This burst mechanism is the source of cellular heterogeneity and stochastic noise [7, 15, 16]. Another crucial mechanism of transcription known as reinitiation [3, 28] is the cause of heterogeneity. This fact has been proven by experiments [3, 6, 9, 29, 30] as well as by recent theories [31–33].

Most of the theories describe GE models using numerical simulations, discrete stochastic models like the Gillespie algorithm [34] and continuous stochastic models involving the chemical Langevin equation (CLE) [35]. The use of the Gillespie algorithm and CLE are limited as they require details of the biochemical reaction kinetics and rate parameters which are often unavailable in the performed biological experiments. Due to these limitations, many biological systems remain unmodeled or modeled without stochastic simulations. One such experiment, carried out by Rossi et al. [36] was not modeled. The authors used a dox-controlled synthetic transcription unit driven by (i) activator only, (ii) repressor only, or (iii) both in an overlapping promoter region. They proposed that the dose-response curve follows the Hill function and the Hill coefficients from the dose-response curves are observed as: 1.6 in the presence of the activator only, 1.8 in the presence of the repressor only, and 3.2 when both the activator and repressor operating together exclusively. Thus, the Hill coefficient goes higher when activator and repressor compete. Rossi et al. [36] suggested that either addition or multiplication of the Hill coefficients 1.6 and 1.8 gives 3.4 and 2.88 (≈ 2.9) respectively, which differs from what they found to be 3.2 (Fig. 1b). Almost a decade later, Yang and Ko [37] proposed a stochastic Markov chain model (MCM) with a three-state activator-repressor system to explain the deviation of observed Hill coefficients from the expected values.

However, both these approaches were unable to explain the collective (Hill coefficient) and stochastic behavior of the three-state competitive activator-repressor system due to the lack of detailed kinetic rates and parameter values. It is thus desirable to explain the model with a proper theory supported by analytical and/or simulation methods. With this as the motivation, accordingly, in this work, we develop a theory that offers detailed chemical kinetics of the competitive activator-repressor system and a most probable set of parameter values that were due for decades. The availability of a suitable analytical theory and the details of reaction kinetics could therefore be powerful tools for future research and analysis of the genetic networks.

In this paper, we consider the competitive binding of TFs (activators and repressors) to the promoter of the gene. There is evidence that activators and repressors can regulate transcription by binding the promoter of a gene mutually exclusively [36]. It has been shown both experimentally [11, 36, 37] and analytically [16, 37] that the competition between activator and repressor molecules to occupy the promoter region can generate a binary response while a graded response is obtained when the molecules act independently separately. However, there is no noise profile¹ available for the transcriptional regulation by the activators and repressors mutually exclusively in the above-mentioned works. Although a few studies in Refs. [38–40], have explored how the competitive binding of TFs in different scenarios influences gene expression noise, nonetheless a general theoretical framework

¹Noise profile is represented by the Fano factor, often called as noise strength. For more please see the glossary.

of noisy behavior of a three-state activator-repressor system still remains unexplored or may stick around in its infancy. Here, we emphasize on studying the noisy behavior of the model and compare its characteristics with a non-competitive activator-repressor model [41]. We will also check the behavior of the architecture in the presence of different activator and repressor molecules instead of doxycycline only.

The paper is organized in the following way. We provide a brief review of the activator-repressor system in Sec. 2. In Sec. 3 we consider the two-state model when only the activator is present. The determination of the promoter activity of the two-state system is provided by model analysis in Subsec. 3.1 and the corresponding parameter estimation is given in Subsec. 3.2. The two-state model with only repressor is discussed in Sec. 4. Next, we consider the competitive regulatory architecture in Sec. 5, wherein the parameter estimation for an activator-repressor system is done in Subsec. 5.1, and the stochastic analysis is carried out in Subsec. 5.2. We compare the competitive and the non-competitive architectures in Sec. 6. The Subsec. 6.1 finds out the role of reinitiation under the action of *aTc* and *GAL* while Subsec. 6.2 explores the effect of noise reducing factors. Finally, in Sec. 7 we discuss the whole study and conclude with the future scopes.

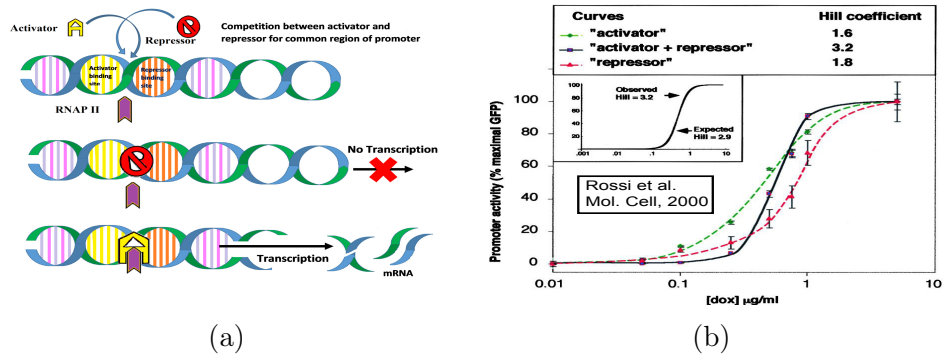


Figure 1: (a) Competition between activator and repressor molecules to bind to a common binding site of the promoter of gene [yellow (red) region indicates activator (repressor) binding site] (b) Rossi et al. [36] experimental plot: promoter activity fitted with the Hill function.

2 Activator-Repressor System: a brief overview

The transcription factors such as activator and repressor molecules can attach to the promoter of the gene and carry out their operation in two ways: either competitively [16] or non-competitively [41].

In this paper, we have discussed the genetic circuits operated by either activator only or repressor only or by both mutually exclusively. Generally, the activator molecules get attached to the promoter of a gene at a specified region known as the activator-binding site (yellow bars in Fig. 1a). They subsequently make the gene ready (active/ON) for transcription by allowing RNAP-II to bind with them. On the other hand, when the repressor molecules occupy their binding site (indicated by red bars in Fig. 1a), they immediately block RNAP-II from sitting on the promoter. As a result, the gene goes into the inactive/OFF state, *i.e.*, inhibits transcription.

In recent work [41], we have rigorously studied the architecture and the noise profile of the non-competitive binding by activator and repressor molecules. The dose (dox)-response (green fluorescent protein/GFP) of an competitive activator-repressor system was experimentally shown in [36] and fitted the parameters with the Hill function. Later, Yang and Ko [37] using stochastic simulation tried to explain the mismatch of the Hill coefficient with the observed experimental data. Furthermore, Karmakar [16] calculates the Probability Distribution Function (PDF) for protein level of a three-state stochastic activator-repressor network and explains the transformation of graded to the binary

response of PDF as observed in the experiment of Rossi et al. [36]. However, none but [16], provide the details of the kinetics and parameters of the system. Clearly, there is a lack of exact parameter values for this network.

To find the parameter values we use a two-state and a three-state genetic network operated by doxycycline as activator and/or repressor. It must be stressed that, the aforementioned works have used networks that show protein synthesis directly from genes and skipped the intermediate transcription stages (mRNA synthesis). Here, we rigorously mention all the possible transitions and parameters involved in the system. However, to fit the parameters with the experimental data, we use the mRNA dynamics instead of protein (one can consider the transcriptional and translational stages have merged to a single stage since it is well known that dynamics followed by mRNA reflect exactly that of the protein multiplied by a scale factor to the magnitudes [32, 33]), as it reduces the number of parameters and their mathematical complexities. Therefore we must multiply some scale factor to the estimated parameter values to fit them with the experimental data (Fig. 6b).

In this study, we observe some interesting dynamical behavior (stochasticity and noise) when both activator and repressor compete mutually for a common binding region of the promoter. In addition, we compare the characteristic differences between this competitive model and a non-competitive model [41].

3 Two-state model when only activator is present

We start with a two-state model [14, 15, 17] (Fig. 2a) where mRNAs may be produced spontaneously from a normal state of gene G_n with a very low leaky basal rate J_0 . The gene can be activated by some inducer (activator), like, doxycycline (Dox) or galactose (GAL) or by some protein produced by the gene itself (positive feedback). The mRNAs are being produced from the active state G_a (ON) at a rate $J_m = J_1$. This mechanism of producing mRNA is called transcription. Protein synthesis starts from the new born mRNAs via rate constant J_p by the process, commonly known as translation. Both mRNAs and proteins degrade by rates k_m and k_p , respectively.

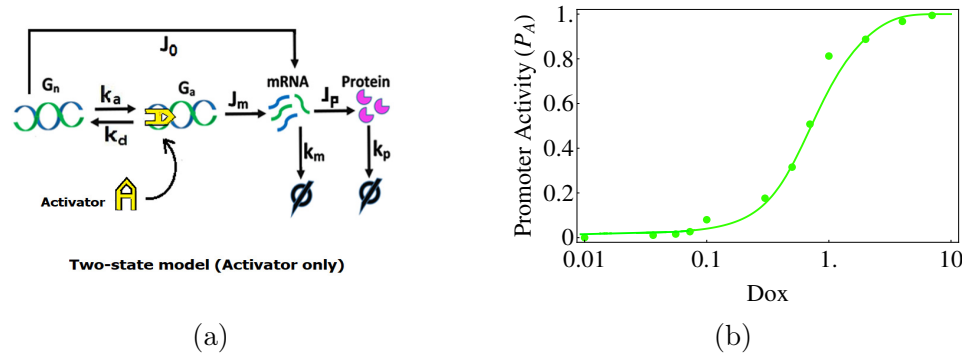


Figure 2: (a) Two-state system where only activator is operating (b) Dose-response curve (solid curve) fitted with experimental data (solid circles) in the presence of activator only (repressor absent) in the promoter of gene.

3.1 Model analysis: determination of promoter activity

The time evolution of mRNA concentration can be expressed deterministically as a function $f(z, G)$ of genetic states (G) as

$$\frac{dz}{dt} = \frac{J_i}{z_{max}} G - k_m z = f(z, G), \quad (1)$$

where $i = 0$ (OFF) or $= 1$ (ON) such that $G = 0$ (gene is inactive) and $G = 1$ (gene is active), respectively. The variable z denotes the concentration of mRNA at time t normalized by the maximum possible mRNA concentration (z_{max}). Here we assume that only stochasticity is involved in the transition of promoter between ON and OFF states.

The probability distribution function (PDF) can be written in the form of the Fokker-Planck equation as

$$\frac{\partial P_i(z, t)}{\partial t} = -\frac{\partial}{\partial z} [f(z, G)P_i(z, t)] + \sum_{j \neq i} k_{ji}P_j(z, t) - k_{ij}P_i(z, t). \quad (2)$$

The first term in RHS is the transport term, second one is the gain term and the last one implies the loss term. Using Eqs. (1) and (2) the Champman-Kolmogorov equation for the reaction scheme of Fig. 2 can be written as

$$\frac{\partial P_0(z, t)}{\partial t} = -\frac{\partial}{\partial z} \left[\left(\frac{J_0}{z_{max}} - k_m z \right) P_0(z, t) \right] + k_d P_1(z, t) - k_a P_0(z, t), \quad (3)$$

$$\frac{\partial P_1(z, t)}{\partial t} = -\frac{\partial}{\partial z} \left[\left(\frac{J_1}{z_{max}} - k_m z \right) P_1(z, t) \right] + k_a P_0(z, t) - k_d P_1(z, t), \quad (4)$$

we have the continuity equation

$$\frac{\partial P}{\partial t} = -\nabla \cdot \mathcal{J}. \quad (5)$$

In the next step, using no flux boundary condition we get the probability current density as

$$\mathcal{J} = \left[\frac{J_i}{z_{max}} - k_m z \right] P_i = 0.$$

Also the steady state condition is given by

$$P(z) = P_1(z) + P_0(z).$$

We have calculated the solution of the coupled Eqs. (3) and (4) as

$$P(z) = C_1 \left(z - \frac{J_0}{k_m z_{max}} \right)^{\frac{k_a}{k_m} - 1} \left(\frac{J_1}{k_m z_{max}} - z \right)^{\frac{k_d}{k_m} - 1}, \quad (6)$$

where, $z_{max} = \frac{J_1 k_a + J_0 k_d}{(k_a + k_d) k_m}$ = steady state mean mRNA.

The normalization constant C_1 can be obtained by integrating $P(z)$ from $z_{min} = \frac{J_0}{k_m}$ to z_{max} , i.e., $\int_{z_{min}=\frac{J_0}{k_m}}^{z_{max}} P(z) dz$.

Now the steady state probability of finding a cell with $z > Z_{th}$, where Z_{th} is a threshold value, is given by

$$P(z > Z_{th}) = 1 - \frac{\int_{z_{min}}^{Z_{th}} P(z) dz}{\int_0^1 P(z) dz} = P_A \text{ (say)}, \quad (7)$$

$$P_A = 1 - \frac{(Z_{th} - J_0)^{k_a} (J_1 - Z_{th})^{k_d} {}_2F_1(Q_1) - (z_{min} - J_0)^{k_a} (J_1 - z_{min})^{k_d} {}_2F_1(Q_2)}{(1 - J_0)^{k_a} (J_1 - 1)^{k_d} {}_2F_1(Q_3) - (-J_0)^{k_a} J_1^{k_d} {}_2F_1(Q_4)}, \quad (8)$$

all the parameters in Eq. (8) are normalized by k_m and here ${}_2F_1(Q_j)$ is the Hypergeometric function given as

$${}_2F_1(Q_1) = {}_2F_1 \left(1, k_a + k_d; k_d + 1; \frac{Z_{th} - J_1}{J_0 - J_1} \right),$$

$$\begin{aligned}
{}_2F_1(Q_2) &= {}_2F_1\left(1, k_a + k_d; k_d + 1; \frac{z_{\min} - J_1}{J_0 - J_1}\right), \\
{}_2F_1(Q_3) &= {}_2F_1\left(1, k_a + k_d; k_d + 1; \frac{J_1 - 1}{J_1 - J_0}\right), \\
{}_2F_1(Q_4) &= {}_2F_1\left(1, k_a + k_d; k_d + 1; \frac{J_1}{J_1 - J_0}\right).
\end{aligned}$$

The probability P_A can also be interpreted as the Promoter activity (% maximal response), defined as the fraction of cells in a cell population with $z > Z_{th}$ [15].

3.2 Parameter Estimation

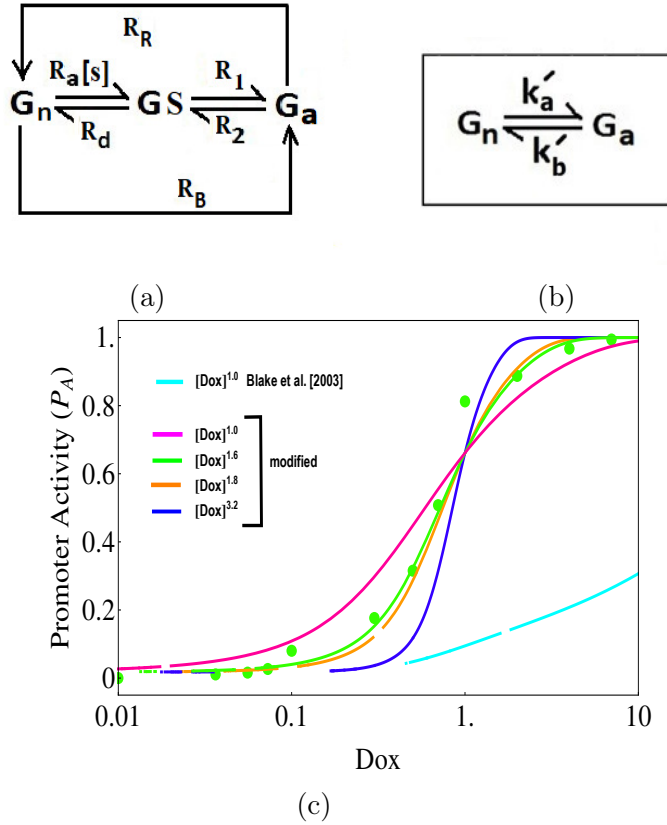


Figure 3: (a) Intermediate state assumption (b) equivalent transition (c) parameter prediction: curves for Dox power = 1.0 (cyan, Blake et al. form [3]), 1.0 (magenta, modified form), 1.6 (green, modified form), 1.8 (orange, modified form) and 3.2 (blue, modified form).

In this section we aim to find the best-fitted parameters for the reaction scheme 2a. In order to do so, we put aside the concept of the Hill function and try to form the GAL-dependent parameters used by Blake et al. [3]. First of all, we theoretically determine the form of the parameters that are responsible for stochasticity in that circuit. In this context, we assume there exists an intermediate state called ‘gene-dox conjugate state’ (GS) between normal state G_n and active state G_a (Fig. 3a). The transition rate constant from G_n to GS carries doxycycline molecule $[S]$, that binds to the gene. Then, with the help of some enzyme (stimuli) or inducer, the gene gets activated (G_a) via rate constant R_1 . The reaction rates R_d and R_2 are the reverse transitions of R_a and R_1 , respectively.

There exists a direct forward transition (R_B) from G_n to G_a and a direct reverse transition (R_R) from G_a to G_n .

The kinetic equations for the reaction scheme in Fig. 3a can be written as (the terms within the parentheses denote molecular concentrations):

$$\frac{d[G_a]}{dt} = R_1[GS] + R_B[G_n] - (R_2 + R_R)[G_a], \quad (9a)$$

$$\frac{d[GS]}{dt} = R_a[S^m][G_n] - R_d[GS] + R_2[G_a] - R_1[GS], \quad (9b)$$

$$\frac{d[G_n]}{dt} = R_d[GS] + R_R[G_a] - (R_a[S^m] + R_B)[G_n], \quad (9c)$$

$$[G_n] + [GS] + [G_a] = 1. \quad (10)$$

Applying the steady state conditions, $\frac{d[G_a]}{dt} = 0$, $\frac{d[GS]}{dt} = 0$, $\frac{d[G_n]}{dt} = 0$, and solving we get,

$$[G_a] = \frac{k'_a}{k'_a + k'_d}, \quad (11)$$

where,

$$k'_a = R_1[R_a[S^m] + \frac{R_B}{R_1}R_d + R_B], \quad (12)$$

$$k'_d = R_2^c[R_a[S^m] + R_d + R_c], \quad (13)$$

with $R_2^c = (R_2 + R_R)$ and $R_c = \frac{R_1 R_R + R_2 R_B}{R_2^c}$.

At this stage of analysis, we further assume that R_R completely unwinds the dox from the gene and hence is a function of $[S]$ such as $R_R = \frac{\alpha}{[S^m]}$, α being a proportionality constant.

When the intermediate state GS is absent, G_a takes the same form as in Eq. (11). Additionally, from the Eq. (12) and (13) we may obtain the exact form of the GAL (dox) dependent rate constants k_a and k_d . In [3], Blake et al. used the GAL-dependent parameters as $k_a = 0.2 \times GAL + 0.02$ and $k_d = 0.1 \times GAL + 0.01 + 0.07/GAL + 0.007/GAL$. We have tried these values and found a curve (cyan in Fig. 3c) nowhere near the experimental data, even though it follows the similar sigmoid nature at much higher GAL concentrations. Therefore we have modified the parameter values a bit and put a power ($m \geq 1$) on dox (or GAL) to make them more general. In order to explain the result found in the experiment performed by Rossi et al. [36], we keep the power of dox as 1.6 for the activator-only model and 1.8 for the repressor-only model. Then, we show that the power goes near to 3.2 when both activator and repressor mutually acts competitively in the circuit. By choosing different numerical values, we have been able to fit the experimental data with theoretical curves quite nicely (Fig. 2b). We have checked by minimizing the relative error and mean squared error to support the robustness of our parameter estimations. The value of parameters for the activator-only model are: $k_a = 1.2 \times S^{1.6} + 0.2$; $k_d = 0.01 \times S^{1.6} + 0.001 + 0.0279/S^{1.6}$; $J_m \in [5 - 250]$; $J_0 = 0.0001$; $k_m = 1$, and $Z_{th} = 0.987$.

4 Two-state model where repressor acts only

We now focus our attention to a two-state repressor only model (Fig. 4a) where mRNA is produced spontaneously from normal state of gene G_n with a very low leaky basal rate J_0 but no mRNA is being produced when the gene is repressed by some TFs, then the gene is assumed to be OFF (G_r).

Whenever a repressor molecule gets attached to the promoter it effectively inhibits the transcription. We may calculate the promoter activity for that model as

$$\begin{aligned}
P(z > Z_{th}) &= 1 - \frac{\int_0^{Z_{th}} P(z) dz}{\int_0^1 P(z) dz}, \\
&= 1 - \frac{Z_{th}^{\frac{k_1}{k_m}} {}_2F_1\left(\frac{k_1}{k_m}, 1 - \frac{k_2}{k_m}; \frac{k_1}{k_m} + 1; \frac{k_1 Z_{th}}{k_1 + k_2}\right)}{{}_2F_1\left(\frac{k_1}{k_m}, 1 - \frac{k_2}{k_m}; \frac{k_1}{k_m} + 1; \frac{k_1}{k_1 + k_2}\right)} = P_R \text{ (say)}.
\end{aligned} \tag{14}$$

Interestingly, by using parameters: $k_1 = 0.02 + 1.8 \times S^{1.8}$; $k_2 = 0.001 + 0.14 \times S^{1.8} + 0.097/S^{1.8}$; $J_0 = 0.0001$; $k_m = 1$ and $Z_{th} = 0.70$, our theoretical plot further agrees well with repression (Fig. 4b) at a particular dox concentration (*i.e.* $S^{1.8}$) found in [36]. By applying gene-dox complex formation, we have estimated these parameter values following the same line of analysis as in the previous section.

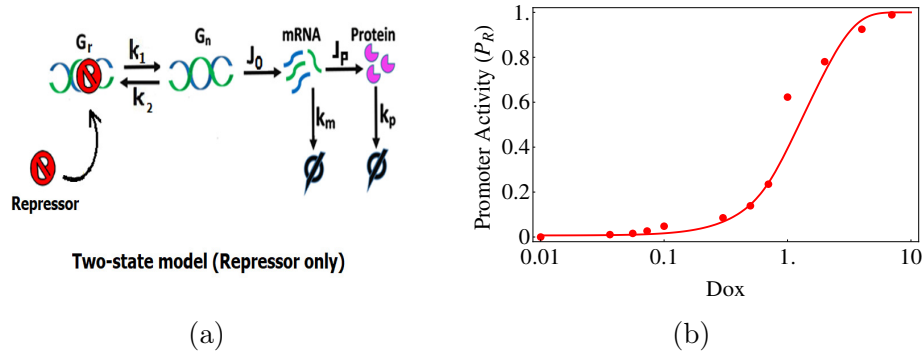


Figure 4: (a) Two-state model where repressor acts solely and inhibits the transcription (b) Dose-response curve (solid curve) fitted with experimental data (solid circles) when only repressor is present (activator absent) in the promoter of gene.

5 Competitive regulatory architecture

There are experimental studies on an eukaryotic transcriptional regulatory network where the activators and repressors bind the same sites of the promoter mutually exclusively [36]. The important feature of the experimental observation is that the activator and repressor concentrations are controlled by the single inducer doxycycline (dox). By varying the dox, the activator and repressor concentrations are varied simultaneously in the experiment. The authors observed an all-or-none response when a combination of activators and repressors act on the same promoter, whereas either alone shows a graded response. The all-or-none and the graded response of an activator-repressor system are explained by considering three states of a gene mainly, inactive (G_r), normal (G_n) and active (G_a), where the activator and repressor compete with each other to bind to the normal state, which is an open state (Fig. 5a) [16]. A successful binding of the activator (repressor) turns the normal state into the active (inactive or repressed) state. Random transitions take place due to random binding and unbinding events of activators and repressors.

In our present analysis we consider the reinitiation of transcription by RNAP II along with the competitive binding events of activators and repressors. The detailed reaction scheme is shown in Fig. 5b.

The promoter activity calculated for the activator-repressor competitive system as

$$\begin{aligned}
P(z > Z_{th}) &= 1 - \frac{\int_0^{Z_{th}} P(z) dz}{\int_0^1 P(z) dz}, \\
&= 1 - \frac{Z_{th}^{\frac{k_{ON}}{k_m}} {}_2F_1\left(1 - \frac{k_{OFF}}{k_m}, \frac{k_{ON}}{k_m}, \frac{k_{ON}}{k_m} + 1; \frac{k_{ON} Z_{th}}{k_{OFF} + k_{ON}}\right)}{{}_2F_1\left(1 - \frac{k_{OFF}}{k_m}, \frac{k_{ON}}{k_m}, \frac{k_{ON}}{k_m} + 1; \frac{k_{ON}}{k_{OFF} + k_{ON}}\right)}, \\
&= P_{AR} \text{ (say)},
\end{aligned} \tag{15}$$

where, ${}_2F_1(a; b; z)$ is a Hypergeometric function.

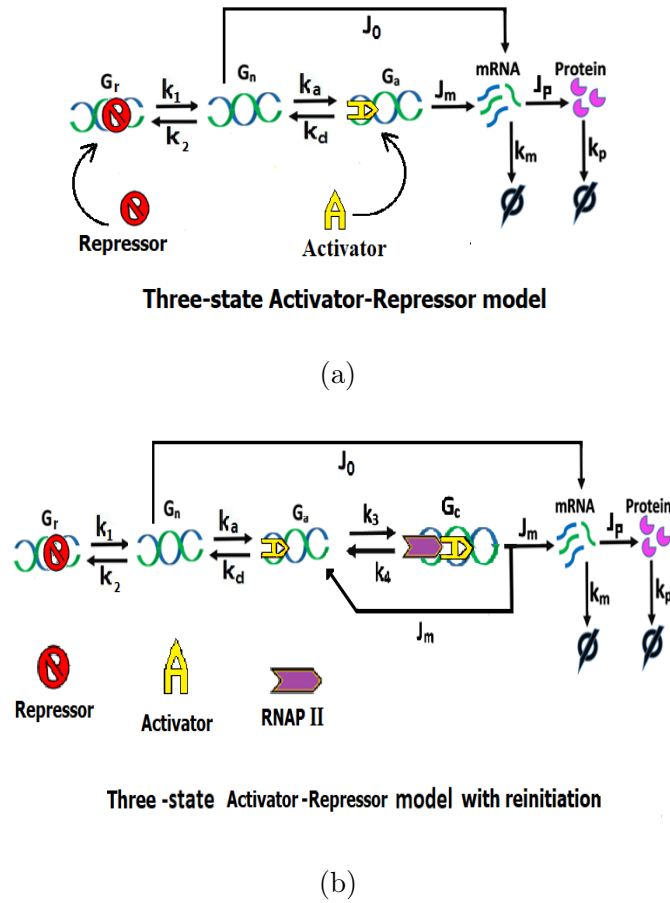


Figure 5: Competitive binding of activator and repressor model (a) without reinitiation, (b) with reinitiation.

5.1 Parameter estimation for Activator-Repressor system

In this section, we attempt to find the possible set of parameters that fits the experimental data of Ref. [36]. They have mentioned in their paper that the dose-response curve obtained from their experiment might follow the Hill function with different Hill coefficients. For different Hill coefficients the model behaves as repressor-only model or activator-only model and a competitive model where both activator and repressor are in competition for binding to the same region of the promoter of gene. In our investigation, we find that the parameter set is much similar to those mentioned by [3] rather than the Hill function. Although in [3] the authors used GAL as activator with power $m = 1.0$

but here we keep the powers of dox (or GAL) as 1.8 for repressor and 1.6 for activator-only following the Hill coefficient values found in [36] (Fig. 6a and Fig. 6b). In order to explore the competitive model we consider a simplified equivalent two-state model (fig. 6d) of reaction scheme 5a. Here, we neglect J_0 in comparison with J_m or J_1 (as $J_0 \ll J_1$).

This assumption does not make any qualitative change in PDF which we have checked explicitly [16]. Moreover, it also holds true in case of mean mRNA and noise strength. It has been known for quite sometime that, the deterministical determination of probability for a three state activator-repressor competitive binding model is very difficult when basal rate J_0 is involved [16]. The deterministic reaction rate equations for reaction scheme shown in fig.5a are given by

$$\frac{d[G_r]}{dt} = k_2[G_n] - k_1[G_r], \quad (16a)$$

$$\frac{d[G_n]}{dt} = k_d[G_a] - k_a[G_n], \quad (16b)$$

$$\frac{d[G_a]}{dt} = k_a[G_n] - k_d[G_a], \quad (16c)$$

$$\frac{d[M]}{dt} = J_1[G_a] + J_0[G_n] - k_m[M], \quad (16d)$$

$$[G_n] + [G_r] + [G_a] = 1. \quad (17)$$

In steady state, $\frac{d[M]}{dt} = 0$ and we have

$$[M] = \frac{J_1[G_a] + J_0[G_n]}{k_m} \simeq \frac{J_1}{k_m}[G_a], \quad (J_0 \ll J_1). \quad (18)$$

Applying the steady state condition, $\frac{d[G_a]}{dt} = 0$, $\frac{d[G_r]}{dt} = 0$, $\frac{d[G_n]}{dt} = 0$ and solving, we get

$$[G_a] = \frac{k_1 k_a}{k_1 k_a + k_d(k_1 + k_2)}. \quad (19)$$

Therefore, Eq. 18 gives

$$[M] = \frac{J_1}{k_m} \frac{k_1 k_a}{k_1 k_a + k_d(k_1 + k_2)}. \quad (20)$$

Now, the reaction rate equations for the simplified equivalent model (see reaction scheme in Fig. 6d) are

$$\frac{d[G_r]}{dt} = k_{OFF}[G_a] - k_{ON}[G_r], \quad (21a)$$

$$\frac{d[M]}{dt} = J_m[G_a] - k_m[M]. \quad (21b)$$

$$[G_r] + [G_a] = 1. \quad (21c)$$

The steady state condition gives

$$[M] = \frac{J_m}{k_m} \frac{k_{ON}}{(k_{ON} + k_{OFF})}, \quad (22)$$

we now write $J_m = J_1$ and compare Eq. (20) with Eq. (22) we get

$$k_{ON} = k_1 k_a, \quad (23)$$

$$k_{OFF} = k_d(k_1 + k_2). \quad (24)$$

Notice that, we get a form of the parameters that have a dominant role over the others for the system. We see that algebraic composition of the component-parameters like k_1, k_a, k_d, k_2 , etc. to form k_{ON} and k_{OFF} actually leads to an addition of powers of dox molecule. Theoretically, we obtain the power of dox (S) for the activator-repressor competitive system as 3.4 which has a close agreement with the experimentally observed value 3.2 (Fig. 6c). Here, by taking the dox-dependent parts of the component-parameters and using Eq. (23) and Eq. (24) we get, $k_{ON} = 1.08 \times S^{3.4}$ and $k_{OFF} = 0.0032 \times S^{3.4} + 0.0027/S^{3.4} + 0.0089 \times S^{0.2} + 0.00097/S^{0.2}$. On top of that, while working with the parameter estimation we notice that besides the power of dox, there are other parameters like Z_{th} that affect the slope of the curves. In our analysis we can put Z_{th} at any value between 70% to 99% to find a best fit curve. We also perform a simulation (shown in Fig. 6a), based on the Gillespie algorithm [34] corresponds to the reaction scheme of Fig. 5a (Pink squares) and Fig. 5b (black stars) respectively, which gives a good agreement to the experimental and as well as the theoretical results. Moreover, to show the robustness of our parameter estimation we examine the sensitivity against the parameters and minimize the standard errors for each data points by using chi-square fitting method (see Appendix-B).

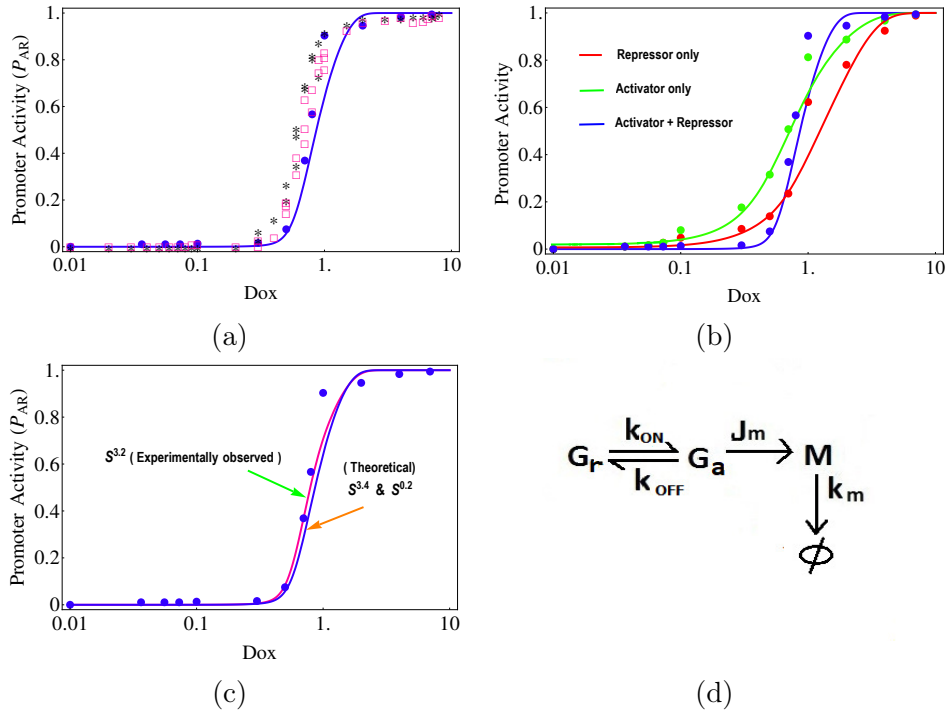


Figure 6: (a) Dose-response curve (solid curve) fitted with experimental data (solid circles) when both activator and repressor compete to sit on the promoter of the gene. Pink squares (Black stars) are obtained by simulation based on the Gillespie algorithm [34] corresponding to the reaction scheme 5a (5b) using $k_3 = 350.0$ and $k_4 = 70.0$ (b) Dose-response curve (solid curves: green- activator-only, red- repressor-only and blue- activator-repressor in competition) fitted with experimental data (solid circles: green- activator-only, red- repressor-only and blue- activator-repressor in competition). (c) Dose-response curve for activator-repressor showing a close agreement of theoretically obtained curve with dox power combination of 3.4 & 0.2 (blue curve) with experimentally found value of 3.2 (pink curve). (d) Two-state equivalent simplified circuit of the three-state activator-repressor competitive model.

5.2 Stochastic Analysis

Let, there are l copy numbers of a particular gene exist in the cell. We consider the reaction scheme in Fig. 5b and let $P(n_1, n_2, n_3, n_4, n_5, t)$ be the probability that at time t , there are n_4 number of

mRNAs and n_5 number of proteins molecules with n_3 number of genes in the initiation complex (G_c), n_2 number of genes in the active state (G_a), and n_1 number of genes in the normal state (G_n). The number of gene in the inactive states (G_r) are thus $(l - n_1 - n_2 - n_3)$. The time evolution of the probability (assuming $J_0 = 0$) is given by

$$\begin{aligned}
\frac{\partial P(n_i, t)}{\partial t} = & k_1[\{l - (n_1 - 1 + n_2 + n_3)\}P(n_1 - 1, n_2, n_3, n_4, n_5, t) \\
& - \{l - (n_1 + n_2 + n_3)\}P(n_i, t)] \\
& + k_2[(n_1 + 1)P(n_1 + 1, n_2, n_3, n_4, n_5, t) - n_1P(n_i, t)] \\
& + k_a[(n_1 + 1)P(n_1 + 1, n_2 - 1, n_3, n_4, n_5, t) - n_1P(n_i, t)] \\
& + k_d[(n_2 + 1)P(n_1 - 1, n_2 + 1, n_3, n_4, n_5, t) - n_2P(n_i, t)] \\
& + k_3[(n_2 + 1)P(n_1, n_2 + 1, n_3 - 1, n_4, n_5, t) - n_2P(n_i, t)] \\
& + k_4[(n_3 + 1)P(n_1, n_2 - 1, n_3 + 1, n_4, n_5, t) - n_3P(n_i, t)] \\
& + J_m[(n_3 + 1)P(n_1, n_2 - 1, n_3 + 1, n_4 - 1, n_5, t) - n_3P(n_i, t)] \\
& + k_m[(n_4 + 1)P(n_1, n_2, n_3, n_4 + 1, n_5, t) - n_4P(n_i, t)] \\
& + J_p[n_4P(n_1, n_2, n_3, n_4, n_5 - 1, t) - n_4P(n_i, t)] \\
& + k_p[(n_5 + 1)P(n_1, n_2, n_3, n_4, n_5 + 1, t) - n_5P(n_i, t)],
\end{aligned} \tag{25}$$

where, $i = 1, 2, \dots, 5$.

We can derive the mean, variance and the Fano factor of mRNAs and proteins from the moments of Eq. (25) with the help of a generating function (Appendix-A). The mean mRNA and protein are given by

$$m^{CWR} = \frac{J_m k_1 k_a k_3}{l_3 k_m}; \quad p^{CWR} = \frac{m^{CWR} J_p}{k_p}. \tag{26}$$

The expression for the Fano factors at mRNA and protein levels are given by

$$FF_m^{CWR} = 1 - m^{CWR} - \frac{J_m k_3 (h_2 k_m + k_1 k_a)}{(k_3 (h_2 (J_m + k_4) - k_1 k_a) + h_8 (k_a (k_d - k_1) - h_2 h_6)) k_m}, \tag{27}$$

$$FF_p^{CWR} = 1 - p^{CWR} + \frac{J_p J_m k_3 (k_m k_p - k_1 k_a)}{l_{10}} + \frac{J_p J_m k_3 (h_2 k_m + k_1 k_a)}{l_{12}} + \frac{J_p}{k_m + k_p}, \tag{28}$$

where

$$\begin{aligned}
l_{12} &= l_1 l_{10} (k_1 k_a (k_3 + l_8) - k_3 l_2 J_m - k_3 k_4 l_2 - k_a k_d l_8 + l_6 l_8 l_2); \\
l_{11} &= l_{10} + l_1 (k_3 J_m - k_1 k_a + k_a k_d + k_3 k_4 - l_4 l_5 - l_4 l_8 - l_6 l_8); \\
l_{10} &= (k_3 l_9 + l_7 (k_a k_d - k_a k_1 - l_4 l_5)) k_p (k_m + k_p); \\
l_9 &= (l_4 (J_m + k_4) - k_1 k_a); \quad l_8 = J_m + k_4 + k_m; \quad l_7 = J_m + k_4 + k_p; \\
l_6 &= k_d + k_3 + k_m; \quad l_5 = k_d + k_3 + k_p; \quad l_4 = k_1 + k_2 + k_a + k_p; \\
l_3 &= k_1 k_a k_3 + (k_1 k_d + k_2 k_d + k_1 k_a) (J_m + k_4); \\
l_2 &= k_1 + k_2 + k_a + k_m; \quad l_1 = (k_m + k_p) k_m k_p.
\end{aligned}$$

For the without-reinitiation scheme (Fig. 5a), the required expression for the mean level of mRNA (m^{CWTR}) and protein (p^{CWTR}) are given by

$$m^{CWTR} = \frac{J_m k_1 k_a}{r_1 k_m}; \quad p^{CWTR} = \frac{m^{CWTR} J_p}{k_p}. \tag{29}$$

The corresponding Fano factors at mRNA (FF_m^{CWTR}) and protein (FF_p^{CWTR}) level are given by

$$FF_m^{CWTR} = 1 - m^{CWTR} + \frac{J_m(r_5 k_m + k_1 k_a)}{r_2 k_m}, \quad (30)$$

$$FF_p^{CWTR} = 1 - p^{CWTR} + X \quad (31)$$

where, $X = \frac{J_p}{k_m + k_p} + \frac{J_p J_m k_1 k_a}{r_9 k_p (k_m + k_p)} + \frac{J_p J_m (r_6 k_m + r_9)}{r_9 (k_m + k_d) (k_m + k_p)} + \frac{J_p J_m k_a k_d (k_m + k_1) r_{10}}{r_4 (k_m + k_d) (k_m + k_p) k_m}$,

$$r_{10} = r_1 + r_3 k_m + r_7 k_p; \quad r_9 = r_6 (k_p + k_d) + k_a (k_1 - k_d); \quad r_8 = r_6 + k_d;$$

$$r_7 = r_8 + k_m; \quad r_7 = r_8 + k_m; \quad r_6 = k_1 + k_2 + k_a + k_p; \quad r_5 = k_1 + k_2 + k_a + k_m;$$

$$r_4 = r_2 (r_8 k_p + r_1); \quad r_3 = r_5 + k_d; \quad r_2 = r_1 + r_3 k_m; \quad r_1 = k_1 k_a + k_1 k_d + k_2 k_d.$$

Here, the superscript ‘C’ stands to indicate the competitive binding, ‘WTR’ represents without-reinitiation and ‘WR’ implies with-reinitiation model.

The experimental values of the rate constants k_i ($i = 1, 2, \dots, 6$) are not yet available for the competitive activator-repressor model (Fig. 5a). In the previous sections, we tried to find a probable set of parameters that fits the experimental data. In this way, the activator and repressor concentrations are controlled by the single inducer doxycycline (dox, denoted by ‘S’). We notice that the theoretically obtained parameter set is quite similar to the parameters used in [3] in a synthetic GAL1* promoter in *Saccharomyces cerevisiae* (commonly known as yeast), except they have used GAL as activator and aTc-bounded tetR as repressor. We check the behavior of the competitive system under the parameter set used in [3] and compare the results with the non-competitive one [41]. The reaction rate constants chosen from [3] for the competitive system are: $k_a = 0.02 + 0.2 \times GAL$, $k_d = 0.01 + 0.1 \times GAL + 0.077/GAL$, $k_3 = 50$, $k_4 = 10$, $k_1 = 10$, $k_2 = 200 \times (tetR)^2/[1 + (C_i \times aTc)^4]^2$, $J_m = 1$, $k_m = 1$, $J_p = 5$, $k_p = 0.0125$, $tetR = 100$, $C_i = 0.1$.

We now study the behavior of mean protein levels and noise strength with respect to the inducer (GAL and aTc) and transcriptional efficiency (refer to glossary), respectively. We note that, the mean protein level varies with GAL and aTc in a similar fashion in the presence and/or absence of reinitiation (Fig. 5a) as in the non-competitive regulatory architecture [41]. The variation of the noise strength with transcriptional efficiency for fixed aTc (500 ng/ml) is again similar to the non-competitive regulatory architecture [41]. Interestingly, the variation of noise strength with transcriptional efficiency for fixed GAL (2%) is different from that obtained from the non-competitive regulatory architecture [41]. We also notice that the noise strength is maximum at the very beginning of the transcriptional efficiency rather than the intermediate level, as shown in Figs. 2c and 2e of [41].

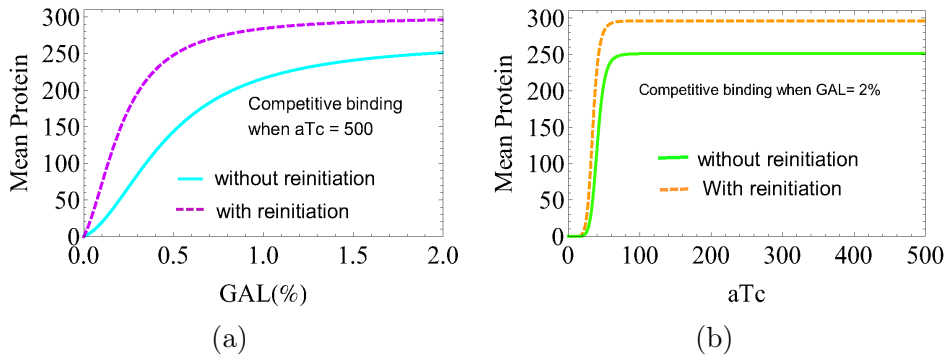


Figure 7: Variation of mean protein: (a) with GAL when aTc is fixed (b) with aTc when GAL is fixed. Solid (dashed) lines are drawn from analytical calculation corresponding to the reaction scheme 5a and 5b respectively. All rate constants are chosen from [3].

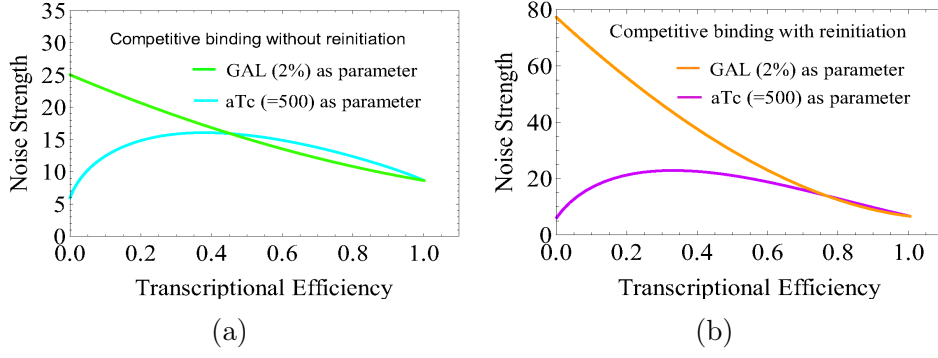
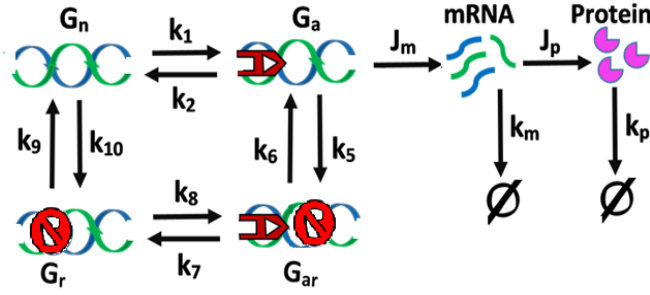


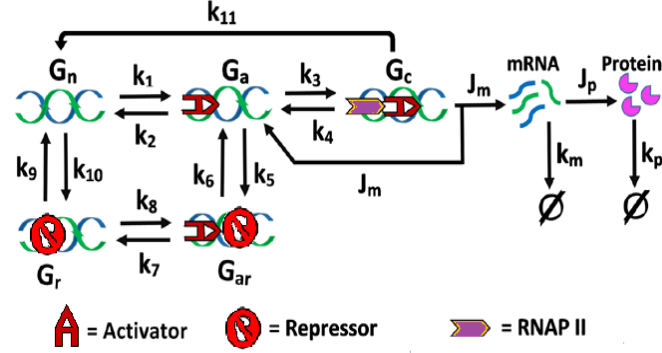
Figure 8: Variation of the noise strength with transcriptional efficiency: (a) green (cyan) line is drawn analytically with 2% GAL concentration (with aTc = 500 ng/ml) from the reaction scheme 5a (b) orange (violet) solid line is drawn analytically with 2% GAL concentration (with aTc = 500 ng/ml) from the reaction scheme 5b, following the same parameter values as used by Blake et al. in [3].

6 Comparison between competitive and non-competitive architecture

In this section, we study the nature of mean products (mRNA/Protein) and their corresponding noise strengths (the Fano factors) for both competitive and non-competitive binding circuits. We first note that, the relative changes of these two physical quantities are clearly visible for both the architectures when the reinitiation is taken under consideration (presented by the dashed lines in characteristic curves). Although the non-competitive circuit and its behaviour were rigorously studied in [41], we put the model diagram here to understand the comparison in a much better way. In a competitive network, the activator and repressor compete for a common binding region of the promoter. As a result, the gene is in either active (ON) or repressed (OFF) state, except a normal state (G_n). Whereas, there could be four possible genetic states: normal (G_n), active (G_a), active-repressed (G_{ar}), and repressed (G_r) as shown in Fig. 9a.



(a)



(b)

Figure 9: Non-competitive binding of activator and repressor (a) without reinitiation (b) with reinitiation and with a reverse transition via k_{11} .

A reverse transition is incorporated via k_{11} from the initiation complex (G_c , arises due to reinitiation) to the normal state (G_n) as there is a possibility of simultaneous unwinding of RNAP-II and activator molecule, that can not be neglected [41]. We find that this reaction path finely affects the mean expression and noise strength of both non-competitive circuit [41] and the competitive one as well.

6.1 Role of reinitiation under the action of aTc and GAL: Anomalous behavior at lower aTc concentration

In this subsection, our focus is centered around some characteristic differences, that appear due to reinitiation when GAL (activator) and aTc (repressor) is operating either competitively or non-competitively, under the same reaction rate constants.

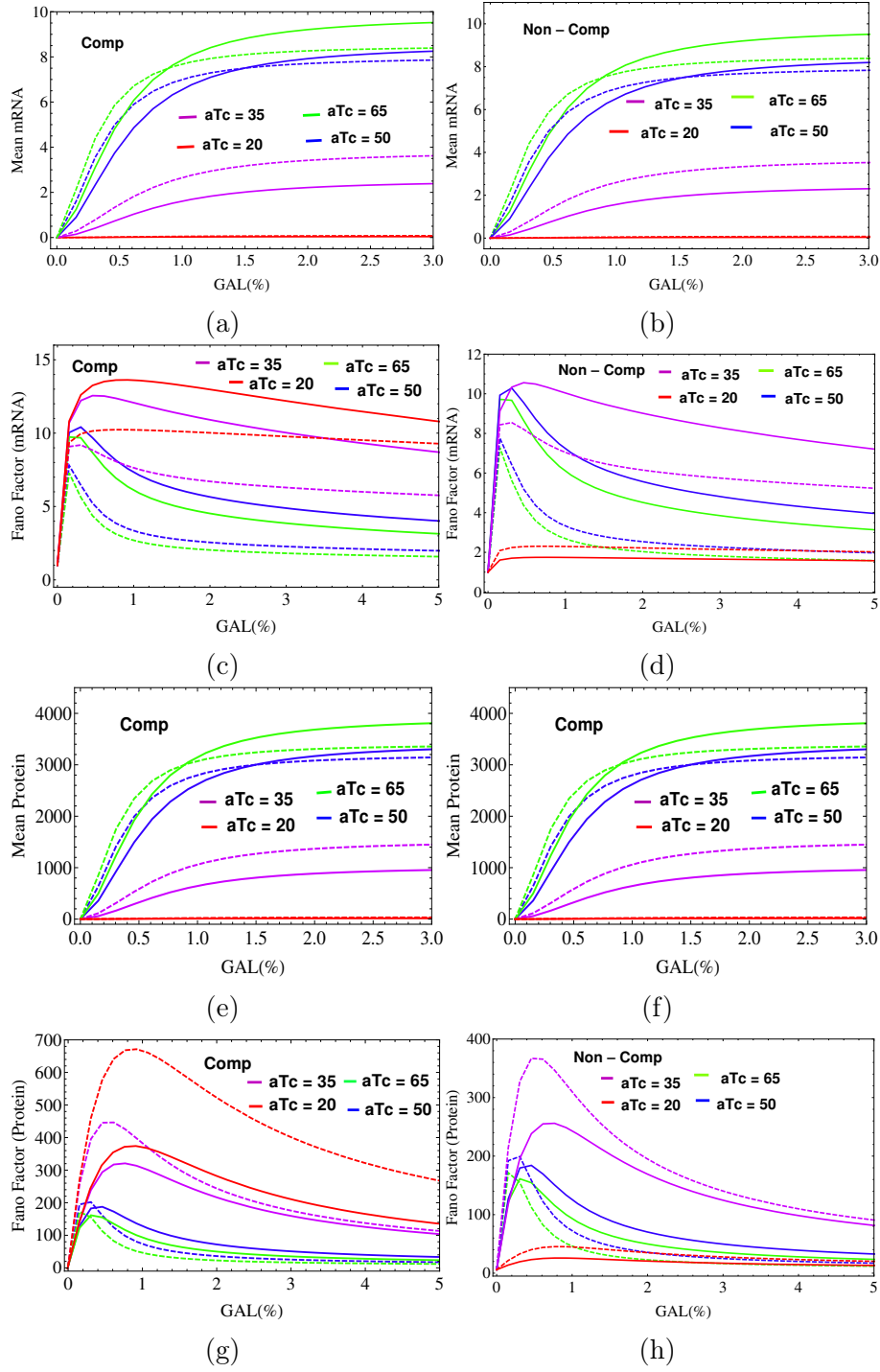


Figure 10: Variation of mean and Fano factor for mRNA and protein level against GAL with different aTc. The solid (dashed) curves correspond to the system without (with) reinitiation for reaction scheme 5a and 9a (5b and 9b). The rate constants are chosen from [3] with $J_m = 15$ and $k_{11} = 0$. abbreviation 'Comp (Non-comp)' implies competitive (non-competitive) model.

In our numerical analysis, we find no observable differences in the variation of mean mRNA as well as mean protein against GAL with different aTc values (colour scheme: aTc = 20, red; aTc = 35, purple; aTc = 50, blue; aTc = 65, green; all units are ng/ml) between both the circuits (Figs. 10a, 10b, 10e and 10f). Rather, they offer the same expression levels under identical rate constants (chosen from [3] with $J_m = 15$ and $k_{11} = 0$). We also notice that the noise strength (the Fano factor) in the super-Poissonian regime ($FF_m > 1$) is higher in the competitive circuit than in non-competitive one

(Figs. 10c,d,g,h and 11c,d,g,h). The findings are summarized below.

- Each solid curve (presenting without-reinitiation) has a point of intersection with the dashed curve (represents with-reinitiation) at a particular GAL value (where, $m^{WR} = m^{WTR}$ and $p^{WR} = p^{WTR}$), beyond which $m^{WR}(\text{or}, p^{WR}) < m^{WTR}(\text{or}, p^{WTR})$. However the curves with $aTc < 45$ ng/ml $m^{WR}(\text{or}, p^{WR}) > m^{WTR}(\text{or}, p^{WTR})$ always holds.
- The curves corresponding to $aTc = 20$ show some anomaly. Usually, $FF_m^{WTR} > FF_m^{WR}$ for all values of aTc in competitive and non-competitive circuits (Fig. 10c, and 10d) as well, except for $aTc = 20$ in non-competitive circuit.
- Only for the competitive model $FF_m^{WTR} > FF_m^{WR}$ while $FF_p^{WTR} < FF_p^{WR}$ for $aTc = 20$ (Fig. 10c and 10g).
- For $aTc > 45$, FF_p^{WR} falls below FF_p^{WTR} , just after attending a quick peak value at lower GAL concentrations.
- The Fano factor, $FF_m(FF_p)$ at $50 < aTc < 65$ rises sharply then gets a certain stability (straight horizontal part) for a very short range of GAL (0.1 - 0.3 unit) and finally falls with increasing GAL. This feature is absent in other values of aTc .

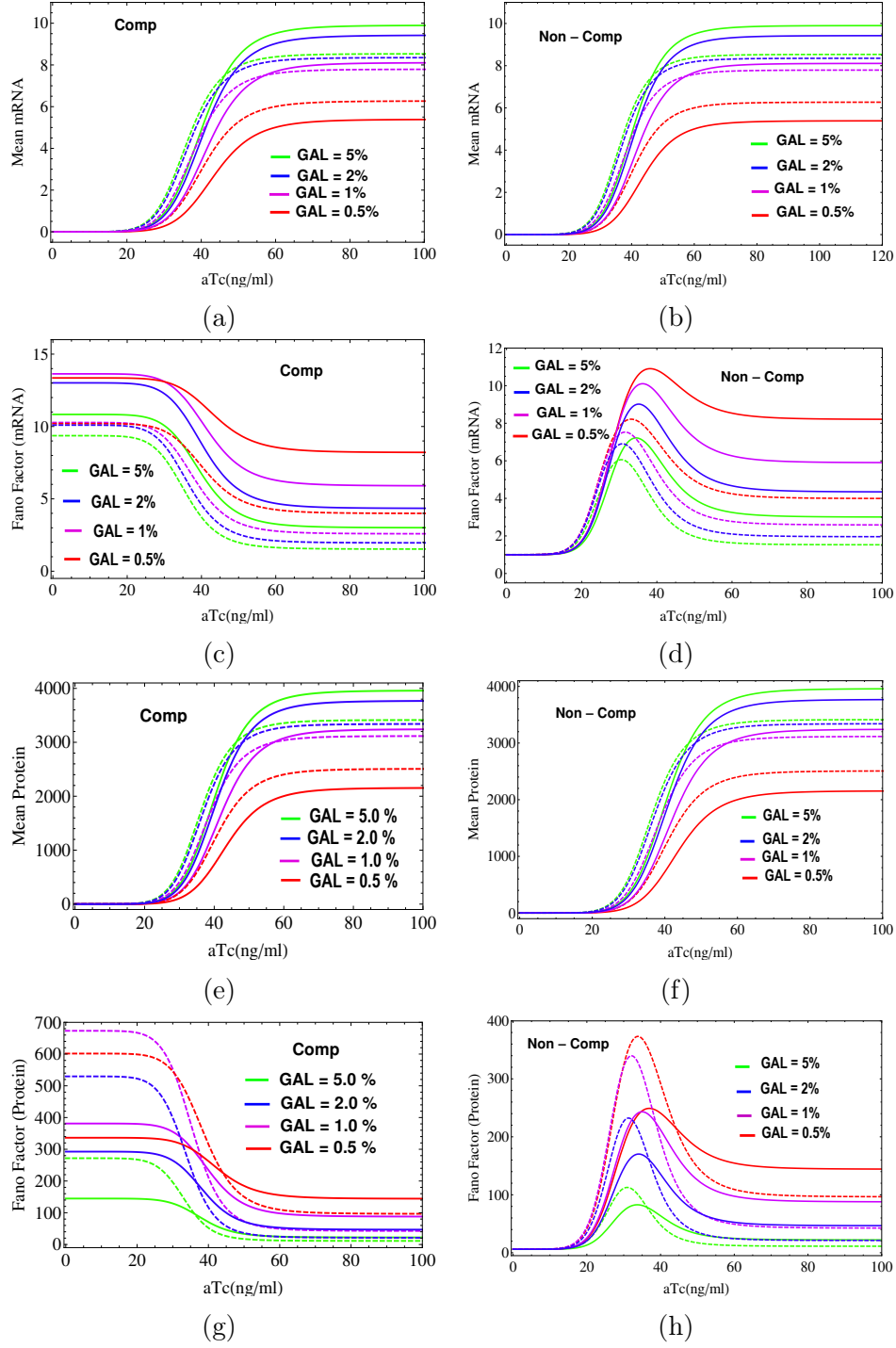


Figure 11: Variation of mean and Fano factor for mRNA and protein level against aTc with different GAL. The solid (dashed) curves correspond to the system without (with) reinitiation for reaction scheme 5a and 9a (5b and 9b). The rate constants are chosen from [3] with $J_m = 15$ and $k_{11} = 0$. abbreviation 'Comp (Non-comp)' implies competitive (non-competitive) model.

The sigmoid nature of the mean expressions with aTc implies that there exist three regions of operation: cut-off, active or sensitive, and saturation [41]. A high value of aTc implies low repression while a lower aTc concentration makes the system OFF due to high repression. The parameters k_2 in the competitive model and k_{10} in the non-competitive model contain *aTc bounded tetR* act as repressor binding rates. We have found some interesting features of mean expressions and the Fano factors varying with aTc for fixed GAL values (colour scheme: GAL = 0.5%, red; GAL = 1.0%, purple; GAL

= 2.0%, blue; GAL = 5.0%, green) for both the models (fig. 11a to 11h). Below are some additional observations that we make from our analysis-

- At the region of sensitivity ($20 \leq aTc \leq 60$), $m^{WR}(or, p^{WR}) > m^{WTR}(or, p^{WTR})$ but $m^{WR}(or, p^{WR}) < m^{WTR}(or, p^{WTR})$ at saturation region ($aTc > 60$), only exception holds for curves with lower GAL concentrations ($\sim 0.5\%$).
- Fig. 11c shows that, $FF_m^{WTR} > FF_m^{WR}$ in all three regions, while this behavior is observed beyond a point of intersection at a certain aTc value for each pair of curves in the non-competitive model (Fig. 11d). We further notice in Fig. 11c that, the noise (WTR) for GAL= 0.5% (solid red curve) is slightly lesser than the noise for GAL= 1.0% (solid purple curve) at the early stages of aTc concentration ($\sim aTc < 35$), after that it goes higher of GAL =1.0% curve for higher aTc values. No such anomaly has been found in the non-competitive system.
- It is noteworthy to mention a major difference that exists in the noise profile for protein level, which arises due to the reinitiation effect. We notice, $FF_p^{WR} \gg FF_p^{WTR}$ at initial values of aTc and at a particular value of aTc each WR curve crosses over the WTR curve. Subsequently WR curve goes below the WTR curve at higher aTc concentrations. A noticeable anomaly is found for Fig. 11g that, curve corresponds to GAL = 0.5% goes slightly lower to the curve for GAL = 1.0% till $aTc \simeq 31.0$ (WTR) and $aTc \simeq 36.0$ (WR) instead of going higher. However, no such anomaly is found in case of non-competitive circuit.
- The amount of noise is higher in competitive circuit than that in non-competitive one.

6.2 Noise reducing factors

We notice that noise can be enhanced or reduced by reinitiation from Fig. 10 and Fig. 11. It is also visible that the competitive binding model shows more noise than the non-competitive one. We now attempt to reduce the noise much below the Poissonian level ($FF_m = 1$). We see, Fig. 12 reveals that it is possible if the value of k_4 is reduced from 10 to 1. According to Blake et al. [3] when $k_4 = 1$ the RNAP-II binds much more tightly with the promoter even when the repressor is rarely present. This results in much reduction of noise for the circuits of both types. Moreover, we find that noise in the competitive model can be reduced more than non-competitive one in the sub-Poissonian region ($FF_m < 1$), corresponding to $k_4 = 10$ (Figs. 12a and 12b) or $k_4 = 1$ (Figs. 12c and 12d).

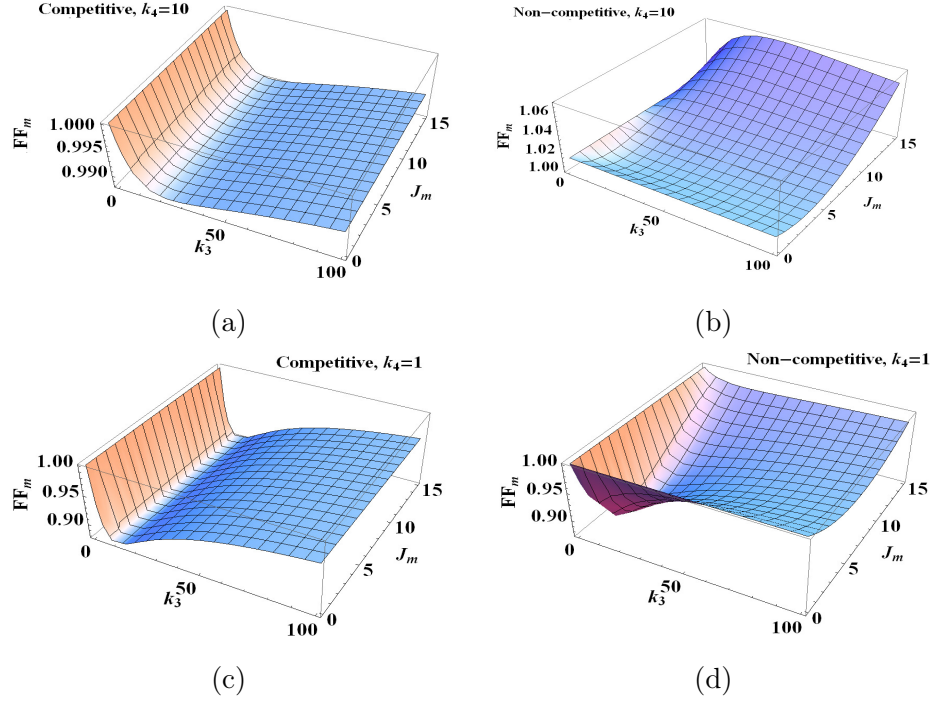


Figure 12: Role of k_4 in reducing noise strength: Variation of the Fano factor at mRNA level with k_3 and J_m (a) competitive circuit with $k_4 = 10$, (b) non-competitive circuit with $k_4 = 10$, (c) competitive circuit with $k_4 = 1$ and (d) non-competitive circuit with $k_4 = 1$. Other parameter values are same as in [3] with $\text{GAL} = 30\%$, $\text{aTc} = 65 \text{ ng/ml}$, $J_m = 15$ and $k_{11} = 0$. These figures are obtained when reinitiation is present in the system.

7 Conclusions and Discussions

The regulation of gene expression through transcription factors (TFs) and control of noise are biologically significant [42–44] to respond to the intra-cellular and external environmental changes as well [25]. They are also important in various medical applications [42–44]. For example, the TFs (activators and repressors) can act as a tumor suppressor in prostate cancer [42]. The noise, arising due to various stochastic events in gene expression is used to modulate the reactivation of HIV from latency (a quiescent state, that is a major barrier to an HIV cure). Noise suppressors stabilize latency while noise enhancers reactivate latent cells [44]. On the contrary, the noisy expression can be beneficial to a population of genetically identical cells by composing phenotypic heterogeneity [6, 10, 23–25].

In this paper, we have studied a gene transcription regulatory architecture where activator and repressor molecules bind the promoter of gene in a competitive fashion. There may be various mode of competition among the TFs and promoter binding sites [16, 38]. Some theoretical studies have explored the kinetics and recorded the effects of TFs on noise [38–40]. Meanwhile, we found an experimental study on a competitive binding network performed by Rossi et al. [36]. Almost a decade later, Yang and Ko [37] tried to explain the experimental results with the help of stochastic simulation. However, both approaches were unable to explain the collective (Hill coefficient) and stochastic behavior of the three-state competitive activator-repressor system because of the lack of detailed kinetics and parameter values. A pioneering work on the same model was done by Karmakar [16], who also found the similar distributions (PDF) as in [36] by theoretical analyses and explained how the response changes from graded to binary in presence of either activator or repressor or both. However, the required parameter values or the exact relationship of the parameters with dox (stimulus) were still unavailable. Moreover, the above-mentioned works did not focus on the noise profile of the three-state

competitive activator-repressor system. In recent work, Braichencho et al. [45] modeled a network where they have studied a proximal promoter-pausing in a three-state activator-repressor system, which can be effectively described by a two-state model in some limiting case. Another competitive model was proposed in [46] where the regulation of gene expression can occur via two cross talking parallel pathways. Although, our approaches and investigations are different in the present work.

The goal of our study is to fabricate a framework to explain the model with a proper theory supported by analytical and/or simulation methods. Consequently, we developed a theory that offers detailed chemical kinetics of the competitive activator-repressor system and a most probable set of parameter values that fit the experimental data [36] quite nicely (Fig. 6b). The dox-dependent parameters, here we found analytically, having very much similar form that proposed earlier in [3] instead of the Hill function [36, 37]. However, in [3] the authors did not clearly mention how the structures of these parameters are formed. Hence, we have designed an analytical treatment by assuming intermediate gene-dox complex formation to determine the exact forms of the parameters (*i.e.* relation with dox) and revealed how the mean expression and noise vary with the changes of these parameter values. The robustness of our parameter estimation is supported by the minimization of relative error and the mean squared error given in Appendix-B. We have found the important parameters that govern the stochastic noise of the circuit. On top of that, we have made a comparison of characteristics between competitive and non-competitive architecture. We have also noticed some anomalous behavior of both mean and the Fano factor with the variation of activator (GAL) and/or repressor (aTc) whenever reinitiation of transcription was taken under consideration. We have noticed that, just as the noise in competitive circuit is high in the super-Poissonian region, its noise can be reduced much lower in the sub-Poissonian regime in comparison with the non-competitive one. However, the mean expression levels remain the same under identical set of rate constants (refer to Fig. 10, 11, and 12). The reason behind such behaviour is subject to further analysis which we have not performed here.

Our proposed theory may be applicable in synthetic biology to understand the architecture of interactions which may buffer the stochasticity inherent to gene transcription of a complex biological system. By using our analytical approach, it is possible to predict the mean and standard deviation of the number of transcribed mRNAs/proteins. There can be further extensive study on the model considering the effect of other parameters that are not considered in present analysis. The availability of a well-designed analytical theory with detailed reaction kinetics of that model could be the powerful tools for future research and analysis for the similar or comparable genetic networks.

Statements and Declarations

Competing Interests: The authors declare that they have no known competing financial interests or personal relationships that could have appeared to influence the work reported in this paper.

Acknowledgment

The authors would like to acknowledge their colleagues and friends for their consistent support and encouragement to this research work.

Glossary

- **Transcription factor:** Transcription factors (TFs) are proteins that have DNA binding domains with the ability to bind to the specific sequences of DNA (called promoter). They control the rate of transcription. If they enhance transcription they are called activators and repressors if they inhibit transcription.

- **Fano factor and Noise strength:** The Fano factor is the measure of deviations of noise from the Poissonian behavior and is defined as [41,45],

$$Fano\ factor\ (mRNA) = \frac{variance\ of\ protein}{mean\ mRNA} = \frac{(standard\ deviation)^2}{mean}.$$

So, for a given mean, smaller the Fano factor implies smaller variance and thus less noise. Therefore, the Fano factor gives a measure of noise strength which is defined (mathematically) as [3],

$$noise\ strength = \frac{variance\ of\ protein}{mean\ mRNA} = \frac{(standard\ deviation)^2}{mean}.$$

So, the Fano factor and noise strength are synonymous.

- **Transcriptional efficiency :** Transcriptional efficiency is the ratio of instantaneous transcription to the maximum transcription [3].

Appendix A

In an attempt to find out the expressions of mean mRNA (protein) and the corresponding Fano factors, we have used a moment generating function which is defined as

$$F(z_i, t) = \sum_{n=0}^{\infty} z_i^{n_i} P(n_i, t). \quad (32)$$

Here, $i = 1, 2, \dots, 5$.

We have,

$$\begin{aligned} \frac{\partial F(z_i, t)}{\partial t} &= \sum_{n=0}^{\infty} z_i^{n_i} \frac{\partial P(n_i, t)}{\partial t}, \\ &= k_1(z_1 - 1) \left[lF - z_1 \frac{\partial F}{\partial z_1} - z_2 \frac{\partial F}{\partial z_2} - z_3 \frac{\partial F}{\partial z_3} \right] \\ &\quad + k_2(1 - z_1) \frac{\partial F}{\partial z_1} + k_a(z_2 - z_1) \frac{\partial F}{\partial z_1} + k_d(z_1 - z_2) \frac{\partial F}{\partial z_2} \\ &\quad + k_3(z_3 - z_2) \frac{\partial F}{\partial z_2} + k_4(z_2 - z_3) \frac{\partial F}{\partial z_3} \\ &\quad + J_m(z_2 z_4 - z_3) \frac{\partial F}{\partial z_3} + k_m(1 - z_4) \frac{\partial F}{\partial z_4} \\ &\quad + J_p(z_5 - 1) z_4 \frac{\partial F}{\partial z_4} + k_p(1 - z_5) \frac{\partial F}{\partial z_5}. \end{aligned} \quad (33)$$

In steady state, $\frac{\partial F(z_i, t)}{\partial t} = 0$ and for total probability, $F(z_i = 1, 0) = 1$.

Now, by setting $\left[\frac{\partial}{\partial z_1} \left(\frac{\partial F}{\partial t} \right) \right]_{z_i=1} = 0$, we get $\frac{\partial F}{\partial z_1} = f_1(\text{say}) = \langle n_1 \rangle = \text{average number of gene at state } G_n$.

similarly, by setting $\left[\frac{\partial}{\partial z_1} \left(\frac{\partial^2 F}{\partial z_1 \partial t} \right) \right]_{z_i=1} = 0$ will give $\frac{\partial^2 F}{\partial z_1^2} = f_{11}(\text{say})$ and so on. Proceeding in the same way we obtain,

$f_5 = \langle n_4 \rangle = \text{mean mRNA}$ and $f_5 = \langle n_5 \rangle = \text{mean Protein}$

$$Fano\ factor\ (mRNA) = \frac{variance\ of\ mRNA}{mean\ mRNA} = \frac{f_{44} + f_4 - f_4^2}{f_4},$$

$$Fano\ factor\ (Protein) = \frac{variance\ of\ Protein}{mean\ Protein} = \frac{f_{55} + f_5 - f_5^2}{f_5},$$

In addition, if the contributions of basal rate J_0 and the reverse transition k_R (or k_{11}) are taken under consideration, there would be two additional terms in Eq. (33) as,

$$J_0(z_4 - z_1) \frac{\partial F}{\partial z_1}, \quad \text{and} \quad k_R(z_1 - z_3) \frac{\partial F}{\partial z_3}.$$

Appendix B

- **Model fitting parameters:** We proposed an analytical theory that fits very much to the experimental result, performed in [36]. The dox-dependent parameters, here we found, having a very similar form, proposed by Blake et al. in [3] instead of Hill type [36, 37]. However, in [3] the authors did not clearly mention how the structures of these parameters are formed. Hence, we design an analytical treatment as described in the main text to determine the forms of the parameters k_a , k_1 , k_2 and k_d . While for the best estimates of other parameters are revised through the minimization of the sum of squared error (SSE) and the mean square error (MSE). We also provide the parameter sensitivity plot in Fig. 13a. Moreover, we calculate and check the relative percentile error (RE) for each curve by using the formula,

$$RE = \frac{y_T - y_E}{y_E} 100\%, \quad (34)$$

where, T stands for theoretical and E stands for experimental.

- **Uncertainty in fitted parameters :** The uncertainty of the parameter estimation, is generally expressed by the mean square errors, is proportional to the SSE (SSWE) and inversely proportional to the square of the coefficient of sensitivity of the model parameters [47]. The mean square fitting error is

$$\sigma^2 = \frac{1}{n - r} \sum_{i=1}^n [w_i(y_T - y_E)]^2 = \frac{Sum\ of\ squared\ weighted\ error}{(n - r)}, \quad (35)$$

where n is the number of observations and r is the number if parameters are being determined. The weighting factor, w_i is determined by the slope of the curve at each data point.

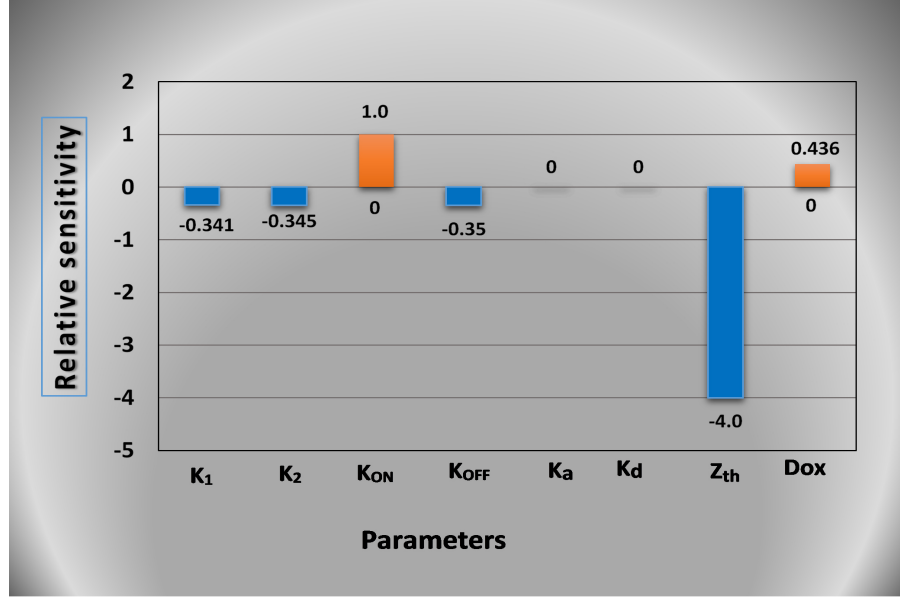
The sensitivity (\mathcal{S}) of a function $f(r)$ over the parameter r is given by

$$\mathcal{S} = \frac{r}{f(r)} \cdot \frac{\partial f(r)}{\partial r}. \quad (36)$$

We obtain the sensitivity of the Fano factor (mRNA) over the fitting parameters and calculate MSE of each parameter keeping others as constant.

$$MSE = \frac{\sigma^2}{\sum_{i=1}^n \left[\frac{\partial f(r)}{\partial r} \right]^2}, \quad (37)$$

where the denominator is the coefficient of sensitivity, squared and summed over all observations.



(a)

Fitting errors and parameter estimations with uncertainties									
Curves for:	For Theoretical curve		Best estimated value of parameter \pm uncertainties						
	SSE	MSE	k_1	k_2	k_a	k_d	k_{ON}	k_{OFF}	Z_{th}
Repressor only	0.0575	0.00479	1.72 \pm 0.159	1.77 \pm 0.554					0.70 \pm 0.02
Activator only	0.0259	0.00216			28.0 \pm 2.916	0.076 \pm 0.0236			0.987 \pm 0.00137
Activator and Repressor competitive	0.0338	0.0026					1.104 \pm 0.0508	0.0059 \pm 0.00408	0.80 \pm 0.0402

(b)

Figure 13: (a) Sensitivity of parameters, (b) Minimized error of fitting and parameter estimation with uncertainties.

We also notice that sensitivity is independent of J_1 , J_0 , k_a and k_d as well. The Z_{th} is the most sensitive parameter and it was kept constant for each case. We found that the promoter activity is sensitive within a small range of values of the chosen parameters. The best parameter estimation and minimization of errors (see Fig. 13b) support the robustness of our result. The square root of the MSE is the standard deviation, and the approximate 95% confidence interval for r is [47]

$$[r]_{95\%} = \mathcal{R} \pm 2\sqrt{MSE}, \quad (38)$$

\mathcal{R} is the best estimate value of parameter r .

References

- [1] Michael B Elowitz, Arnold J Levine, Eric D Siggia, and Peter S Swain. Stochastic gene expression in a single cell. *Science*, 297(5584):11831186, 2002.
- [2] Ertugrul M Ozbudak, Mukund Thattai, Iren Kurtser, Alan D Grossman, and Alexander Van Oudenaarden. Regulation of noise in the expression of a single gene. *Nature genetics*, 31(1):6973, 2002.
- [3] William J Blake, Mads Kærn, Charles R Cantor, and James J Collins. Noise in eukaryotic gene expression. *Nature*, 422(6932):633637, 2003.
- [4] Jonathan M Raser and Erin K O’shea. Noise in gene expression: origins, consequences, and control. *Science*, 309(5743):20102013, 2005.
- [5] Ido Golding, Johan Paulsson, Scott M Zawilski, and Edward C Cox. Real-time kinetics of gene activity in individual bacteria. *Cell*, 123(6):10251036, 2005.
- [6] William J Blake, Gábor Balázsi, Michael A Kohanski, Farren J Isaacs, Kevin F Murphy, Yina Kuang, Charles R Cantor, David R Walt, and James J Collins. Phenotypic consequences of promoter-mediated transcriptional noise. *Molecular cell*, 24(6):853865, 2006.
- [7] Arjun Raj, Charles S Peskin, Daniel Tranchina, Diana Y Vargas, and Sanjay Tyagi. Stochastic mrna synthesis in mammalian cells. *PLoS biology*, 4(10):e309, 2006.
- [8] David M Suter, Nacho Molina, David Gateld, Kim Schneider, Ueli Schibler, and Felix Naef. Mammalian genes are transcribed with widely different bursting kinetics. *science*, 332(6028):472-474, 2011.
- [9] Caroline R Bartman, Nicole Hamagami, Cheryl A Keller, Belinda Giardine, Ross C Hardison, Gerd A Blobel, and Arjun Raj. Transcriptional burst initiation and polymerase pause release are key control points of transcriptional regulation. *Molecular cell*, 73(3):519532, 2019.
- [10] Mukund Thattai and Alexander Van Oudenaarden. Stochastic gene expression in fluctuating environments. *Genetics*, 167(1):523530, 2004.
- [11] Stephen R Biggar and Gerald R Crabtree. Cell signaling can direct either binary or graded transcriptional responses. *The EMBO journal*, 20(12):31673176, 2001.
- [12] Archie Paulson, Shijie Zhong, and John Wahr. Modelling post-glacial rebound with lateral viscosity variations. *Geophysical Journal International*, 163(1):357371, 2005.
- [13] Álvaro Sánchez and Jané Kondev. Transcriptional control of noise in gene expression. *Proceedings of the National Academy of Sciences*, 105(13):5081-5086, 2008.
- [14] Vahid Shahrezaei and Peter S Swain. Analytical distributions for stochastic gene expression. *Proceedings of the National Academy of Sciences*, 105(45):17256 -17261, 2008.
- [15] Rajesh Karmakar and Indrani Bose. Graded and binary responses in stochastic gene expression. *Physical biology*, 1(4):197, 2004.
- [16] Rajesh Karmakar. Conversion of graded to binary response in an activator-repressor system. *Physical Review E—Statistical, Nonlinear, and Soft Matter Physics*, 81(2):021905, 2010.

- [17] Niraj Kumar, Thierry Platini, and Rahul V Kulkarni. Exact distributions for stochastic gene expression models with bursting and feedback. *Physical review letters*, 113(26):268105, 2014.
- [18] Lacramioara Bintu, Nicolas E Buchler, Hernan G Garcia, Ulrich Gerland, Terence Hwa, Jané Kondev, and Rob Phillips. Transcriptional regulation by the numbers: models. *Current opinion in genetics & development*, 15(2):116124, 2005.
- [19] Lacramioara Bintu, Nicolas E Buchler, Hernan G Garcia, Ulrich Gerland, Terence Hwa, Jane Kondev, Thomas Kuhlman, and Rob Phillips. Transcriptional regulation by the numbers: applications. *Current opinion in genetics & development*, 15(2):125135, 2005.
- [20] Thomas Kuhlman, Zhongge Zhang, Milton H Saier Jr, and Terence Hwa. Combinatorial transcriptional control of the lactose operon of escherichia coli. *Proceedings of the national academy of sciences*, 104(14):60436048, 2007.
- [21] Jose MG Vilar and Stanislas Leibler. DNA looping and physical constraints on transcription regulation. *Journal of molecular biology*, 331(5):981989, 2003.
- [22] Jose MG Vilar and Leonor Saiz. DNA looping in gene regulation: from the assembly of macromolecular complexes to the control of transcriptional noise. *Current opinion in genetics & development*, 15(2):136144, 2005.
- [23] Mads Kaern, Timothy C Elston, William J Blake, and James J Collins. Stochasticity in gene expression: from theories to phenotypes. *Nature Reviews Genetics*, 6(6):451464, 2005.
- [24] Arjun Raj and Alexander Van Oudenaarden. Nature, nurture, or chance: stochastic gene expression and its consequences. *Cell*, 135(2):216226, 2008.
- [25] Bruce Alberts, Alexander Johnson, Julian Lewis, Martin Ra, Keith Roberts, and Peter Walter. Helper t cells and lymphocyte activation. In *Molecular biology of the cell*. 4th edition. Garland Science, 2002.
- [26] Mark Ptashne. Regulation of transcription: from lambda to eukaryotes. *Trends in biochemical sciences*, 30(6):275279, 2005.
- [27] Kevin Struhl. Fundamentally different logic of gene regulation in eukaryotes and prokaryotes. *Cell*, 98:14, 1999.
- [28] Bo Liu, Zhanjiang Yuan, Kazuyuki Aihara, and Luonan Chen. Reinitiation enhances reliable transcriptional responses in eukaryotes. *Journal of The Royal Society Interface*, 11(97):20140326, 2014.
- [29] Wanqing Shao and Julia Zeitlinger. Paused RNA polymerase ii inhibits new transcriptional initiation. *Nature genetics*, 49(7):10451051, 2017.
- [30] Natalya Yudkovsky, Jerey A Ranish, and Steven Hahn. A transcription reinitiation intermediate that is stabilized by activator. *Nature*, 408(6809):225229, 2000.
- [31] Zhixing Cao, Tatiana Filatova, Diego A Oyarzún, and Ramon Grima. A stochastic model of gene expression with polymerase recruitment and pause release. *Biophysical Journal*, 119(5):1002 1014, 2020.
- [32] Rajesh Karmakar. Control of noise in gene expression by transcriptional reinitiation. *Journal of Statistical Mechanics: Theory and Experiment*, 2020(6):063402, 2020.

- [33] Rajesh Karmakar and Amit Kumar Das. Effect of transcription reinitiation in stochastic gene expression. *Journal of Statistical Mechanics: Theory and Experiment*, 2021(3):033502, 2021.
- [34] Daniel T Gillespie. Exact stochastic simulation of coupled chemical reactions. *The journal of physical chemistry*, 81(25):23402361, 1977.
- [35] CW Gardiner. *Handbook of stochastic methods for physics, chemistry, and the natural sciences* springer. Berlin (4th Ed), 2009.
- [36] Fabio MV Rossi, Andrew M Kringstein, Albert Spicher, Oivin M Guicherit, and Helen M Blau. Transcriptional control: rheostat converted to on/off switch. *Molecular cell*, 6(3):723728, 2000.
- [37] Hsih-Te Yang and Minoru SH Ko. Stochastic modeling for the expression of a gene regulated by competing transcription factors. *PloS one*, 7(3):e32376, 2012.
- [38] Dipjyoti Das, Supravat Dey, Robert C Brewster, and Sandeep Choubey. Eect of transcription factor resource sharing on gene expression noise. *PLOS Computational Biology*, 13(4):e1005491, 2017.
- [39] Anat Burger, Aleksandra M Walczak, and Peter G Wolynes. Influence of decoys on the noise and dynamics of gene expression. *Physical Review E—Statistical, Nonlinear, and Soft Matter Physics*, 86(4):041920, 2012.
- [40] M Soltani, P Bokes, Z Fox, and A Singh. Nonspecific transcription factor binding can reduce noise in the expression of downstream proteins. *Physical biology*, 12(5):055002, 2015.
- [41] Amit Kumar Das. Stochastic gene transcription with non-competitive transcription regulatory architecture. *The European Physical Journal E*, 45(7):61, 2022.
- [42] Jerrey A Magee, Sarki A Abdulkadir, and Jerrey Milbrandt. Haploinsuciency at the *nkx3. 1* locus: a paradigm for stochastic, dosage-sensitive gene regulation during tumor initiation. *Cancer cell*, 3(3):273283, 2003.
- [43] Leor S Weinberger, John C Burnett, Jared E Toettcher, Adam P Arkin, and David V Schaffer. Stochastic gene expression in a lentiviral positive-feedback loop: Hiv-1 *tat* fluctuations drive phenotypic diversity. *Cell*, 122(2):169182, 2005.
- [44] Roy D Dar, Nina N Hosmane, Michelle R Arkin, Robert F Siliciano, and Leor S Weinberger. Screening for noise in gene expression identifies drug synergies. *Science*, 344(6190):13921396, 2014.
- [45] Svitlana Braichenko, James Holehouse, and Ramon Grima. Distinguishing between models of mammalian gene expression: telegraph-like models versus mechanistic models. *Journal of the Royal Society Interface*, 18(183):20210510, 2021.
- [46] Feng Jiao and Chunjuan Zhu. Regulation of gene activation by competitive cross talking pathways. *Biophysical journal*, 119(6):12041214, 2020.
- [47] Laurence H Smith, Peter K Kitanidis, and Perry L McCarty. Numerical modeling and uncertainties in rate coecients for methane utilization and tce cometabolism by a methane-oxidizing mixed culture. *Biotechnology and Bioengineering*, 53(3):320331, 1997.